

Photosynthetic Control of Arabidopsis Leaf Cytoplasmic Translation Initiation by Protein Phosphorylation

Edouard Boex-Fontvieille¹, Marlène Daventure², Mathieu Jossier¹, Michel Zivy², Michael Hodges¹, Guillaume Tcherkez^{1,3*}

1 Institut de Biologie des Plantes, CNRS UMR 8618, Saclay Plant Sciences, Université Paris-Sud, Orsay, France, **2** Plateforme PAPPSO, UMR de Génétique Végétale, Ferme du Moulon, Gif sur Yvette, France, **3** Institut Universitaire de France, Paris, France

Abstract

Photosynthetic CO₂ assimilation is the carbon source for plant anabolism, including amino acid production and protein synthesis. The biosynthesis of leaf proteins is known for decades to correlate with photosynthetic activity but the mechanisms controlling this effect are not documented. The cornerstone of the regulation of protein synthesis is believed to be translation initiation, which involves multiple phosphorylation events in Eukaryotes. We took advantage of phosphoproteomic methods applied to *Arabidopsis thaliana* rosettes harvested under controlled photosynthetic gas-exchange conditions to characterize the phosphorylation pattern of ribosomal proteins (RPs) and eukaryotic initiation factors (eIFs). The analyses detected 14 and 11 new RP and eIF phosphorylation sites, respectively, revealed significant CO₂-dependent and/or light/dark phosphorylation patterns and showed concerted changes in 13 eIF phosphorylation sites and 9 ribosomal phosphorylation sites. In addition to the well-recognized role of the ribosomal small subunit protein RPS6, our data indicate the involvement of eIF3, eIF4A, eIF4B, eIF4G and eIF5 phosphorylation in controlling translation initiation when photosynthesis varies. The response of protein biosynthesis to the photosynthetic input thus appears to be the result of a complex regulation network involving both stimulating (e.g. RPS6, eIF4B phosphorylation) and inhibiting (e.g. eIF4G phosphorylation) molecular events.

Citation: Boex-Fontvieille E, Daventure M, Jossier M, Zivy M, Hodges M, et al. (2013) Photosynthetic Control of Arabidopsis Leaf Cytoplasmic Translation Initiation by Protein Phosphorylation. PLoS ONE 8(7): e70692. doi:10.1371/journal.pone.0070692

Editor: Thomas Preiss, The John Curtin School of Medical Research, Australia

Received: April 2, 2013; **Accepted:** June 20, 2013; **Published:** July 24, 2013

Copyright: © 2013 Boex-Fontvieille et al. This is an open-access article distributed under the terms of the Creative Commons Attribution License, which permits unrestricted use, distribution, and reproduction in any medium, provided the original author and source are credited.

Funding: The authors thank the Institut Fédératif de Recherche 87 for its financial support for phosphoproteomics. E. B.-F. thanks the Labex Saclay Plant Science for its support through a post-doctoral grant. GT and MH thank the Agence Nationale de la Recherche for supporting running costs of this study, thanks to a project Jeunes Chercheurs, under contract no. 08-330055. The funders had no role in study design, data collection and analysis, decision to publish, or preparation of the manuscript.

Competing Interests: The authors have declared that no competing interests exist.

* E-mail: guillaume.tcherkez@u-psud.fr

Introduction

Intense efforts are currently devoted to disentangle the regulation of protein biosynthesis in plant organs with the aim to increase the protein fraction or the nitrogen content in crops. In addition to nitrogen nutrition, metabolic commitments and transcriptional control, mRNA translation is believed to be of importance to regulate protein synthesis and protein content of plant tissues. Plants are phototrophic organisms and thus their translational activity is strongly influenced by light and photosynthesis. Pioneering studies with isotopic labeling showed that in mature leaves, gross protein synthesis (incorporation of ¹⁵N in proteins) was larger in the light than in the dark [1] and in *Chlorella pyrenoidosa* (single celled green alga), steady-state photosynthesis has been found to be associated with ¹⁴C-labeling in proteinaceous amino acids [2]. More recently, molecular studies have shown that in plant leaves, light stimulates translational activity of photosynthesis-related mRNA (ferredoxin) [3] and furthermore, a larger fraction of polysomal ribosomes has been found in the light compared to the dark [4]. In leaves, isotopic labelling (¹⁴CO₂) has demonstrated that an increasing proportion (from 10 to 24% of net fixed carbon) of carbon is allocated to protein synthesis as photosynthesis increases from low to high [CO₂] conditions, demonstrating a positive effect of photosynthetic input (CO₂ mole

fraction) on gross protein synthesis [5]. Nevertheless, little is known about the mechanisms by which photosynthesis influences translation and overall protein production.

Quite generally, protein phosphorylation appears to play a crucial role in the regulation of translational initiation. A key-step of translational control seems to be the phosphorylation of the ribosomal protein S6 (RPS6), since alterations of its phosphorylation level have drastic effects on growth and polysome formation [6,7]. Recent proteomic characterization of ribosomal phosphorylation patterns showed a significant increase of the phosphorylation level of RPS6 as well as two other ribosomal proteins (RPP1 and RPL29-1) in the light when compared to the dark [8]. RPS6 is known to be phosphorylated by S6 kinase (S6K) which in turn may be phosphorylated by other kinases such as PDK1 and the TOR/RAPTOR complex [9,10]. Translation initiation in the cytoplasm begins with the recognition of the cap structure (5' end of mRNA) by the initiation factors eIF4E, eIF4G, eIF4B and the RNA helicase eIF4A. The 40S ribosomal subunit binds an eIF2-containing complex (eIF2, GTP and Met-tRNA) and the initiation factors eIF1, eIF1A, eIF3 and eIF5, forming the 43S initiation complex. The cap-binding complex interacts with the 43S initiation complex and allows mRNA scanning and the correct positioning at the start codon. eIF5B eventually promotes joining of the 60S ribosomal subunit. At each of these steps,

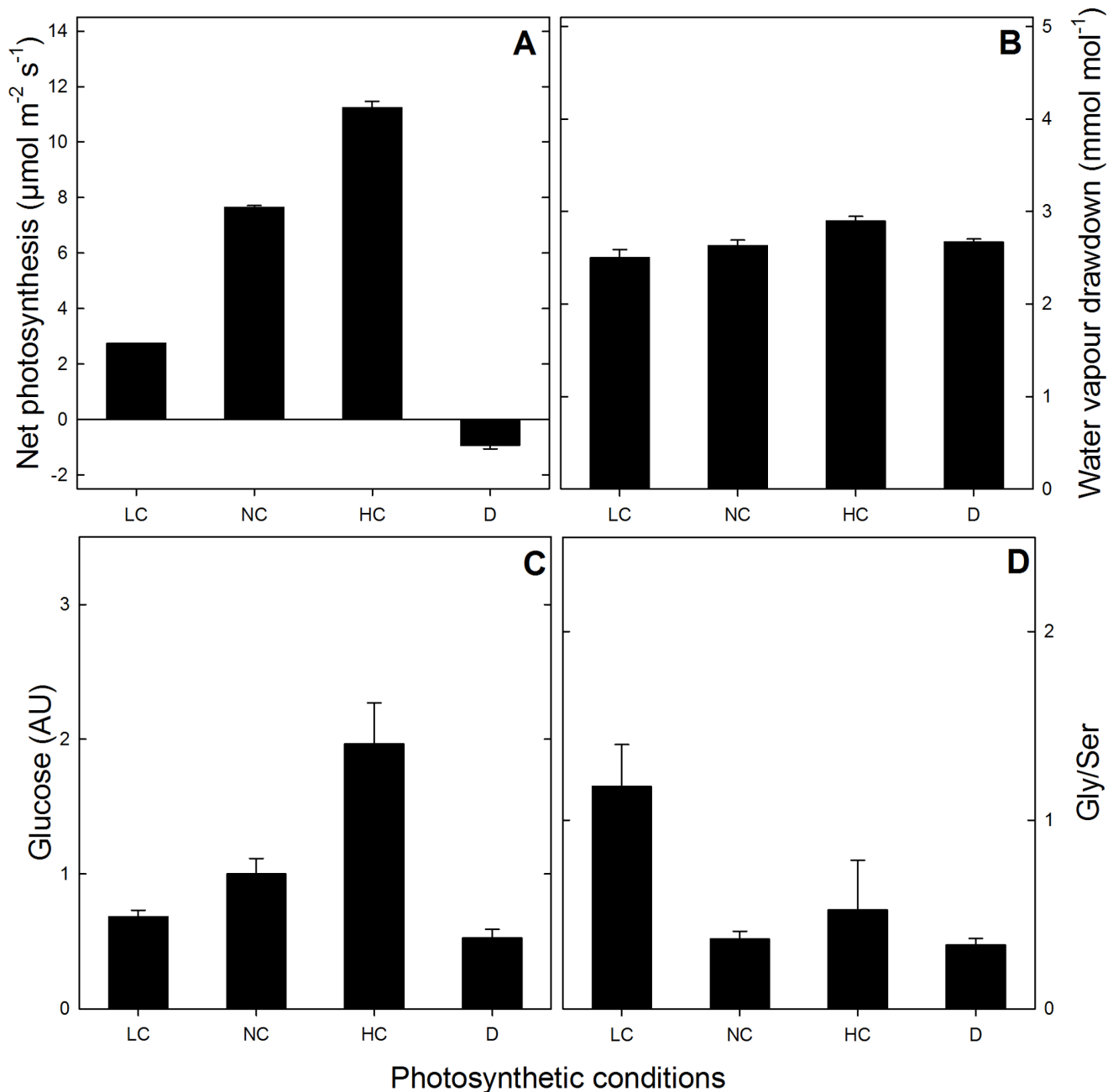


Figure 1. Photosynthetic parameters. leaf net photosynthesis (A), leaf-to-air water vapour drawdown (B), leaf glucose content (C) and Gly-to-Ser ratio (D), under the different photosynthetic contexts used (LC, NC and HC: 100, 380 and 1000 $\mu\text{mol mol}^{-1} \text{CO}_2$; D: darkness). doi:10.1371/journal.pone.0070692.g001

eIF-phosphorylation is crucial for the control of initiation and there are multiple phosphorylation sites on these proteins, which can either stimulate or repress translation (for a review, see [11]). The phosphorylation of eIF1, eIF2 β , eIF3c and eIF5 by CK2 favours the assembly of the complex that binds the 40S ribosomal subunit *in vitro* [12,13]. Phosphorylation of eIF4B and poly-A binding protein (PABP) promotes their interaction and the formation of a circular mRNA structure that stimulates translation initiation [14]. In mammalian cells, the alteration of eIF4E phosphorylation compromises mRNA cap recognition, however if eIF4E phosphorylation occurs in plants the equivalent phosphorylated Ser residue in the primary sequence is missing [15].

Similarly, eIF4G and eIF(iso)4G, which participate to mRNA binding and interact with eIF4B, might be controlled by phosphorylation but this is at present uncertain due to the absence of the phosphorylation motif for binding the MNKI kinase [16]. Phosphorylation of eIF2 α by GCN2 seems to down-regulate translation by disfavoured the eIF2B-catalyzed exchange of GDP for GTP [16,17]. The current knowledge of this complex orchestration mostly stems from *in vitro* studies, characterization of mutants or use of stressful conditions (e.g., anoxia). But quite critically, the way by which eIF phosphorylation is influenced by natural light/dark conditions and photosynthetic conditions is not well documented.

As an aid in clarifying the nature and the phosphorylation of molecular actors involved in photosynthesis-driven translational control, we have investigated the phosphorylation of ribosomal proteins and initiation factors in *Arabidopsis* leaves in different photosynthetic contexts: various CO₂ conditions (ordinary [CO₂] (380 ppm), high [CO₂] (1000 ppm), low [CO₂] (100 ppm)) in the light and ordinary CO₂ in the dark. We took advantage of a gas-exchange system with liquid N₂ spraying for instant sampling and nanoLC-MS/MS based phosphoproteomics to characterize phosphorylated peptides in rosette leaves. We report 11 new phosphorylation sites in eIF proteins and 14 new sites in ribosomal proteins (RPs), describe significant CO₂-dependent protein phosphorylation patterns and show concerted changes in 13 eIF phosphorylation sites and 9 ribosomal phosphorylation sites. Our results suggest a key role of eIF and RP phosphorylation in photosynthesis-driven regulation of mRNA translation in leaves.

Results

Photosynthetic Conditions and Sampling

Short-day grown *Arabidopsis* rosettes were placed in a purpose-built chamber connected to a gas-exchange system, as described in the *Material and Methods*. CO₂ and water vapour (H₂O) were monitored so as to calculate photosynthesis and transpiration. After four hours at a photosynthetic steady-state at the desired CO₂ mole fraction, leaf rosettes were sprayed with liquid nitrogen and sampled. Sampling in the dark was carried out on dark-adapted leaves, that is, after two hours in darkness following 4 hours of steady photosynthesis at ordinary CO₂ (380 ppm). Protein composition and phosphorylation were analysed by nanoLC-MS/MS. Figures 1A and 1B show steady net photosynthesis rates and leaf-to-air water vapour draw-down levels, respectively. There was a very clear effect of CO₂ on photosynthesis demonstrating that the four types of samples analysed here (ordinary, low and high CO₂ and darkness) corresponded to strongly different photosynthetic contexts. This CO₂ effect was independent from water deficit since the water vapour draw-down between evaporation sites and atmosphere remained constant (Figure 1B). Photosynthetic metabolism (photosynthate production) was reflected by the glucose content which correlated with the photosynthesis rate (Figure 1C). The quotient of the two key photorespiratory metabolites Gly and Ser, which correlates with O₂ fixation (photorespiration activity), was indeed higher at low CO₂ (Figure 1D, LC).

LC-MS Analysis of Leaf Proteins

For proteomic characterization, protein samples were digested by trypsin and then analysed as described in [18]. Peptides were methylated via formylation with labeled (deuterated) or non-labeled formaldehyde and reduction with cyanoborohydride. Non-labeled and labeled peptides were mixed (the condition of interest (non-labeled) and the mix of all samples as a reference (labelled) mixed with a 1:1 mixing ratio, see *Material and methods*), and underwent a SCX (Strong Cation Exchange) chromatography. Collected fractions were enriched in phospho-peptides by IMAC (Immobilized ion Metal Affinity Chromatography) and then analysed by nanoLC-MS/MS. The quantity of proteins was determined by direct analysis (no SCX and labeling). (Phospho)peptides were identified with X!Tandem [19] and quantified with MassChroQ [20]. Table 1 summarizes the number of phosphopeptides identified using nanoLC-MS/MS, with the complete list of phosphorylated peptide sequences in Table S1. 156 ribosomal proteins were detected, among which 33 phosphorylated ribosomal proteins were found, represented

by 45 phosphopeptides (for a complete description of RP and eIF proteins identified, see Table S2). 25 eIFs were detected, with 15 phosphorylated proteins represented by 28 phosphopeptides. The statistical analysis of peptide quantity in samples (three independent biological replicates were analysed for each experimental condition) indicated no difference between the CO₂ and dark treatments. Therefore, the changes in phosphopeptide abundance described below are strictly related to changes in the phosphorylation ratio.

Phosphopeptides and Phosphorylation Sites

Phosphopeptides identified in RPs and eIFs are listed in Table 1, in which significant (i.e., with statistically significant changes under photosynthetic/light conditions), insignificant and punctual (i.e., punctually phosphorylated with little repeatability) sites are distinguished. Phosphorylation sites were mapped using MS spectra and searching with the MASCOT engine, thus giving obvious phosphorylated residues in peptides. In some instances, however, ambiguous cases occurred, in which the nature of the phosphorylated residue could not be determined (two undistinguishable possibilities). This was the case for peptides from RPS6A/RPS6B, RPS2C, RPS17 and eIF4G that include two phosphorylatable Ser residues or both Ser and Thr residues (Table S2). New phosphorylation sites (absent from PhosPhAt 4.0 (<http://phosphat.mpimp-golm.mpg.de/>) and from [21] and [8]) were detected in at least 16 ribosomal proteins, including in the ribosomal proteins RPS6A and/or RPS6B at Ser 229 (with mono- and bis-phosphorylated peptides DRRpS²²⁹ESLAK and DRRpS²²⁹Eps²³¹LAK, respectively, Figure 2). In this case, the specific nature of the ribosomal protein RPS6A or B could not be solved due to their close sequence identity. We also detected a new phosphopeptide located in the activation loop of the S6 kinases S6K1 and S6K2 (SNpS²⁹⁰MCGTTEYMAPEIVR). Other new sites located in eIFs are listed in Table 1 and amongst them, the most significant are Ser 178 (or Thr 177) and Ser 530 in eIF4G (Figure 2). We did not detect any phosphorylated sites in eIF4E and PABP (Poly-A Binding Proteins). Amongst the components of the eIF2B complex (a guanidine nucleotide exchange factor which catalyzes the substitution of hydrolysed GDP for GTP in eIF2), no phosphopeptide was detected for eIF2B α , eIF2B γ and eIF2B ϵ while eIF2B β was phosphorylated at Ser 173 (SADKSpS¹⁷³LTR) and eIF2B δ in 10 different Ser residues (Table 1).

Phosphorylation Patterns

Nine phosphorylation sites in ribosomal proteins and 13 phosphorylation sites in eIFs were significantly affected ($P < 0.04$) by conditions: light/dark and/or photosynthetic activity (CO₂ mole fraction). Their phosphorylation patterns are shown in Figures 3 and 4. Several phosphorylation sites in ribosomal proteins were affected by both light/dark and photosynthesis conditions, such as Ser 229 and 231 in RPS6A and/or RPS6B, Ser 19 in RPS14A and Thr 138 in RPL13D (Figure 3A and 3B). In the latter case, the photosynthetic effect was not monotonous and light decreased Thr 138 phosphorylation (at 380 ppm CO₂). Most sites in eIFs were significantly affected by light/dark conditions, except for eIF4B1 at Ser 480; by contrast, this site was significantly affected by CO₂ mole fraction. Most sites were positively influenced by CO₂ mole fraction (i.e. there was a positive correlation between phosphorylation and photosynthetic activity), except for eIF4G, eIF4A and eIF5A (Figure 4A). That is, the components of eIF4F were either not phosphorylated in our conditions (eIF4E) or responded negatively to photosynthetic conditions (eIF4G, eIF4A). 17 and 5 sites in ribosomal proteins and eIFs, respectively, were

Table 1. Eukaryotic ribosomal protein and initiation factor phosphopeptides identified by nanoLC-MS/MS.

Protein	Gene locus	Phosphopeptides identified ^a	Phosphorylation sites	New sites ^b	Significant sites ^c	Insignificant sites	Sites punctually detected ^d
RPS2C	At2g41840	3	2	1	0	Ser 258, Ser 273 or Thr 275 or Ser 276	0
RPS3aA	At3g04840	2	2	0	0	Ser 69, Ser 236	0
RPS3aA, RPS3aB	At3g04840, At4g34670	1	1	1	0	0	Ser177
RPS6A	At4g31700	7	4	0	Ser 237, Ser 240, Ser 247	0	Ser 249
RPS6B	At5g10360	4	2	0	Ser 237, Ser 240	0	0
RPS6A, RPS6B	At4g31700, At5g10360	3	2	1	Ser 229, Ser 231	0	0
RPS9B	At5g15200	1	1	0	0	0	Ser 68
RPS10A	At4g25740	1	1	1	0	0	Ser116
RPS14A	At2g36160	1	1	1	Ser 19	0	0
RPS14B	At3g11510	1	1	0	0	Ser 19	0
RPS17	At1g79850	1	1	0	0	0	Thr 115 or Ser 117
RPS27A, RPS27B, RPS27C	At2g45710, At3G61110, At5g47930	1	1	0	0	Ser 29	0
RPP0B	At3g09200	1	1	0	0	Ser 305	0
RPP0C	At3g11250	1	1	0	0	Ser 308	0
RPP1A, RPP1C	At1g01100, At5g47700	1	1	1	0	0	Ser 10
RPP1A, RPP1B, RPP1C	At1g01100, At4g00810, At5g47700	2	1	0	0	Ser 102	0
RPP2A	At2g27720	1	1	1	0	Ser 95	0
RPP2B	At2g27710	1	1	1	0	Ser 80	0
RPP2A, RPP2B, RPP2D	At2g27720, At2g27710, At3g44590	2	1	0	0	Ser 120	0
RPP3A, RPP3B	At4g25890, At5g57290	2	1	0	0	0	Ser 90
RPL3A	At1g43170	3	3	3	0	Ser 28	Ser 139, Ser 377
RPL6B, RPL6C	At1g74060, At1g74050	1	1	1	0	Ser 52	0
RPL11A, RPL11B, RPL11C, RPL11D	At2g42740, At3g58700, At4g18730, At5g45775	1	1	0	0	Thr 46	0
RPL13D	At5g23900	1	1	0	Thr 138	0	0
50S ribosomal protein L1	At363490	1	2	1	0	0	Ser32, Ser 35
RACK1B	At1g48630	1	1	1	0	0	Ser 285
eIF5	At1g77840	1	1	0	0	0	Ser 201
eIF5A2	At1g26630	2	1	0	Ser 2	0	0
eIF5A3	At1g69410	2	1	1	Ser 2	0	0
eIF4A1	At3g13920	1	1	0	Ser 4	0	0
eIF4A1, eIF4A2	At3g13920, At1g13020	1	1	0	Thr 145	0	0

Table 1. Cont.

Protein	Gene locus	Phosphopeptides identified ^a	Phosphorylation sites	New sites ^b	Significant sites ^c	Insignificant sites	Sites punctually detected ^d
eIF4A3	At1g72730	1	1	0	Thr 147	0	0
eIF4B1	At3g26400	3	3	1	Ser 480	Ser 462	Thr 239
eIF4B2	At1g13020	5	5	3	Ser 475, Ser 489	Thr 283, Ser 493	Ser 136
eIF4G	At3g60240	7	7	3	Thr 177 or Ser 178, Ser 178	0	Ser 530, Ser 710, Ser 1353, Ser 1508, Ser 1527
eIF3B1, eIF3B2	At5g27640, At5g25780	2	2	1	Ser 684	Ser 273	0
eIF3 subunit 7	At4g20980	1	1	0	Thr 74	0	0
eIF3 subunit 7	At5g44320	1	1	1	Thr 70	0	0
eIF3c1	At3g56150	1	1	1	Ser 40	0	0
eIF2B beta	At3g07300	1	1	1	0	Ser 173	0
eIF2B delta	At5g38640	10	9	3	Ser 127	Ser 108, Ser 220	Ser 88, Ser 91, Ser 93, Ser 126 or Ser 127, Ser 141 or Ser 142 or Ser 143, Ser 218 or Thr 219 or Ser 220
TruB	At5g14460	1	1	0	Ser 132	0	0
TOTAL		85	73	29	24	23	26

a- Phosphopeptides sequences are listed in Table S2.

b- A phosphorylation site is considered as new when absent from refs. [8] and [11] and PhosphAt 4.0 database (<http://phosphat.mpimp-golm.mpg.de/>).

c- Phosphorylation patterns are presented in Figures 3 and 4.

d- By 'punctually', we mean occasional detection of phosphorylation, with no clear pattern.

doi:10.1371/journal.pone.0070692.t001

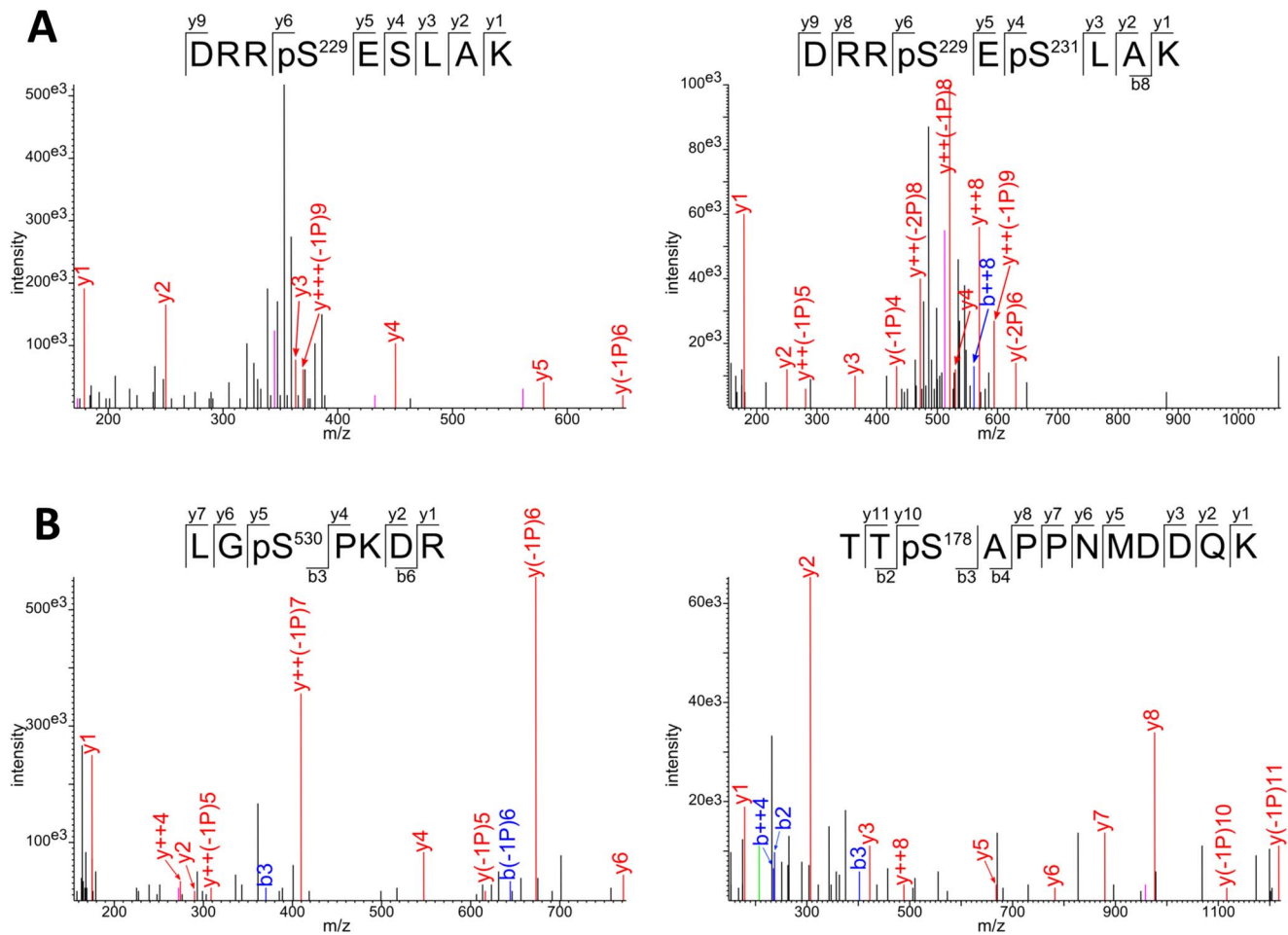


Figure 2. Identification of Ser 229 and Ser 231 in RPS6A/B (A) and Ser 178 and Ser 530 in eIF4G (B) by mass spectrometric sequencing of two phosphorylated peptides. Spectra of methylated and phosphorylated peptides show b (N-terminal) and y (C-terminal) fragment-ions as displayed in the sequence (top of each spectrum). Lower case p indicates the phosphate group. Phosphorylation is localized according to the pattern of the fragment-ions containing phosphate and fragment-ions with phosphate loss. Ions showing a neutral loss of H_3PO_4 and $2 \times \text{H}_3\text{PO}_4$ are labelled with “-1P” and “-2P” respectively. Fragment from neutral losses are coloured in pink, and fragment ions are coloured in green. Parental ion fragments are, as shown in insets: DRRpSEpSLAK (m/z 643.31177, $z=2$), DRRpSESLAK (m/z 402.55502, $z=3$), LGpSPKDR (m/z 458.75925, $z=2$) and TTpSAPPNMDQK (m/z 724.83307, $z=2$). They were identified in 6, 20, 1 and 76 spectra, respectively. doi:10.1371/journal.pone.0070692.g002

constantly phosphorylated, with no significant change with light/dark or CO_2 mole fraction. For example, this was the case of Ser 52 in RPL6C and Ser 4 in eIF4A1 (Table S1). The pseudo-uridylylase (TruB, enzyme which post-transcriptionally isomerizes uridine residues in t-RNA) was affected by light/dark conditions (more phosphorylated at night at Ser 132) but not by photosynthesis, while eIF2B δ at Ser 127 was contrarily affected (more phosphorylated in the light, significant photosynthetic effect) and eIF2B β (Ser 173) was not significantly affected by any condition. That is, the phosphorylation pattern of the eIF2B complex did not appear to be simple, with contrasted effects on individual subunits.

Discussion

The phosphorylation status of eIFs and RPs is known to be crucial in regulating protein interactions and activity for translation initiation [11]. Here, we show multiple phosphorylation sites and protein phosphorylation patterns affected by light and photosynthetic (CO_2) conditions.

RP Phosphorylation

In eukaryotic cellular systems examined so far (mammals, yeast and plants), cytosolic RPs have been found to be phosphorylated, allowing a fine control of translation. RPS6 activity seems to be controlled by phosphorylation (for a review, see [22]). In mammalian cells, the TOR kinase phosphorylates the S6K kinase that in turn phosphorylates RPS6. Homologs of TOR and S6K exist in plants and RPS6 has indeed been found to be phosphorylated [23,24]. A recent investigation of RP phosphorylation in *Arabidopsis* leaves in the light and in the dark has further shown that RPP1A/B/C, RPS6A/B, RPP0B, RPS2C and RPL29A are phosphorylated and RPP1A/B/C, RPS6A/B, and RPL29A respond to light/dark conditions: RPS6A/B appeared to be significantly more phosphorylated in the light while RPP1A/B/C and RPL29A appeared to be slightly but insignificantly more phosphorylated in the light [8]. Here, we show that in addition to RPP1A/B/C, RPS2C, RPP0C and RPS6A/B, 25 other ribosomal proteins can be phosphorylated (Table 1), among which two are significantly affected by light (RPS14A and RPL13D). The phosphorylation of RPs of the small subunit (RPS6 and RPS14)

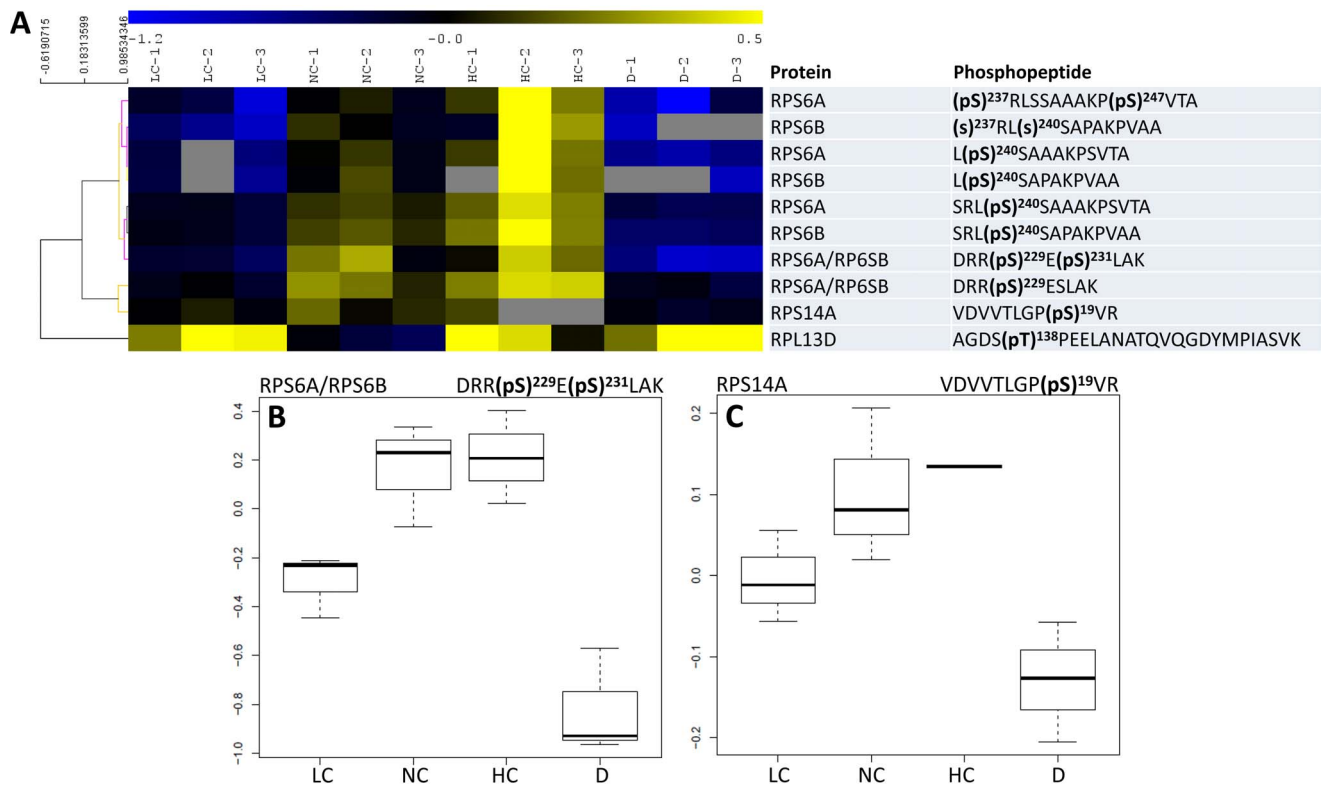


Figure 3. Phosphorylation pattern of ribosomal proteins. **A**, Heat map representation of the phosphorylation level of significant phosphopeptides (phosphorylated peptides that showed statistically significant changes with conditions). A hierarchical clustering analysis is shown on the left. All significant phosphopeptides had a very similar pattern, except for RPL13D, which was minimally phosphorylated under ordinary conditions (NC). Unavailable data (non-detected peptides) are indicated with a grey cell. **B** and **C**, Detailed phosphorylation pattern of RPS6A/B and RPS14A. LC, NC, HC and D: low, normal and high CO₂ and darkness. doi:10.1371/journal.pone.0070692.g003

further appeared to correlate with photosynthetic activity (Figure 3). Changes in phosphorylation of RPs caused by environmental or hormonal conditions have been found to occur in maize roots under hypoxia [23] and anticipated in plant lines with altered TOR or S6K kinases [9,25]. During the light period and photosynthesis, which are associated with an increased translation activity (see *Introduction*), the stimulation of translational activity is thus likely to be associated with a pronounced phosphorylation of RPs, thereby promoting the formation of the initiation complex.

eIF Phosphorylation

The phosphorylation of several eIFs is believed to be of considerable importance in triggering translation initiation [26,27]. Multiple phosphorylations of several eIFs by CK2 are required for the formation of the mRNA-binding complex containing eIF4A, eIF4B, eIF4F and eIF5 [12]. To date, eIF4A has been found to be increasingly phosphorylated and eIF4B dephosphorylated in response to stressful environmental changes in plant cells [28,29,30]. eIF3c has been shown to be phosphorylated by CK2 [13] although no apparent effect of eIF3c phosphorylation on translation has been detected [31].

Here, we show that several eIF3 (eIF3a, eIF3b, eIF3c), eIF4 (eIF4A, eIF4B, eIF4G) and eIF5 (eIF5A2, eIF5A3) proteins are phosphorylated and many phosphorylation sites responded significantly to light/dark and photosynthesis conditions (Figure 4). Importantly, eIF4A and eIF4G were found to be less phosphorylated at high photosynthetic rates and more

phosphorylated in the dark. It is plausible that eIF4A and eIF4G phosphorylation inhibits day-time translation or that the phosphorylation is not required under ordinary, non-stressful conditions (or alternatively, that photosynthate deprivation in the dark causes eIF4A and eIF4G phosphorylation). All phosphorylation sites of eIF4B respond positively to photosynthesis suggesting a reverse pattern (eIF4B phosphorylation required for ordinary translation). In our study, eIF4E, eIF(iso)4E and eIF(iso)4G did not appear to be phosphorylated, despite the fact that their involvement has proven important in selecting translated mRNAs [32]. eIF3c, eIF5A2 and eIF5A3 were found to be more phosphorylated in the light compared to the dark, with little photosynthetic effect. The interaction of eIF3c with eIF5 is believed to be crucial for AUG recognition along the mRNA and therefore, these eIFs (and eIF3c phosphorylation at Ser 40) are probably essential at all times when translation is active (daytime). We further show that other eIF3s are phosphorylated (eIF3B1/2), implying that eIF3 activity might also require phosphorylation at other sites. It should nevertheless be recognized that phosphorylation of eIF5A has been found to favour eIF5A sequestration in the nucleus and thus it has been hypothesized to repress translation [33,34]. The individual effects of multiple phosphorylation events in eIFs on translation are thus presently difficult to appreciate but here, the clear effect on RPS6 and eIF4B phosphorylation undoubtedly reflects translation enhancement at increased photosynthetic rates.

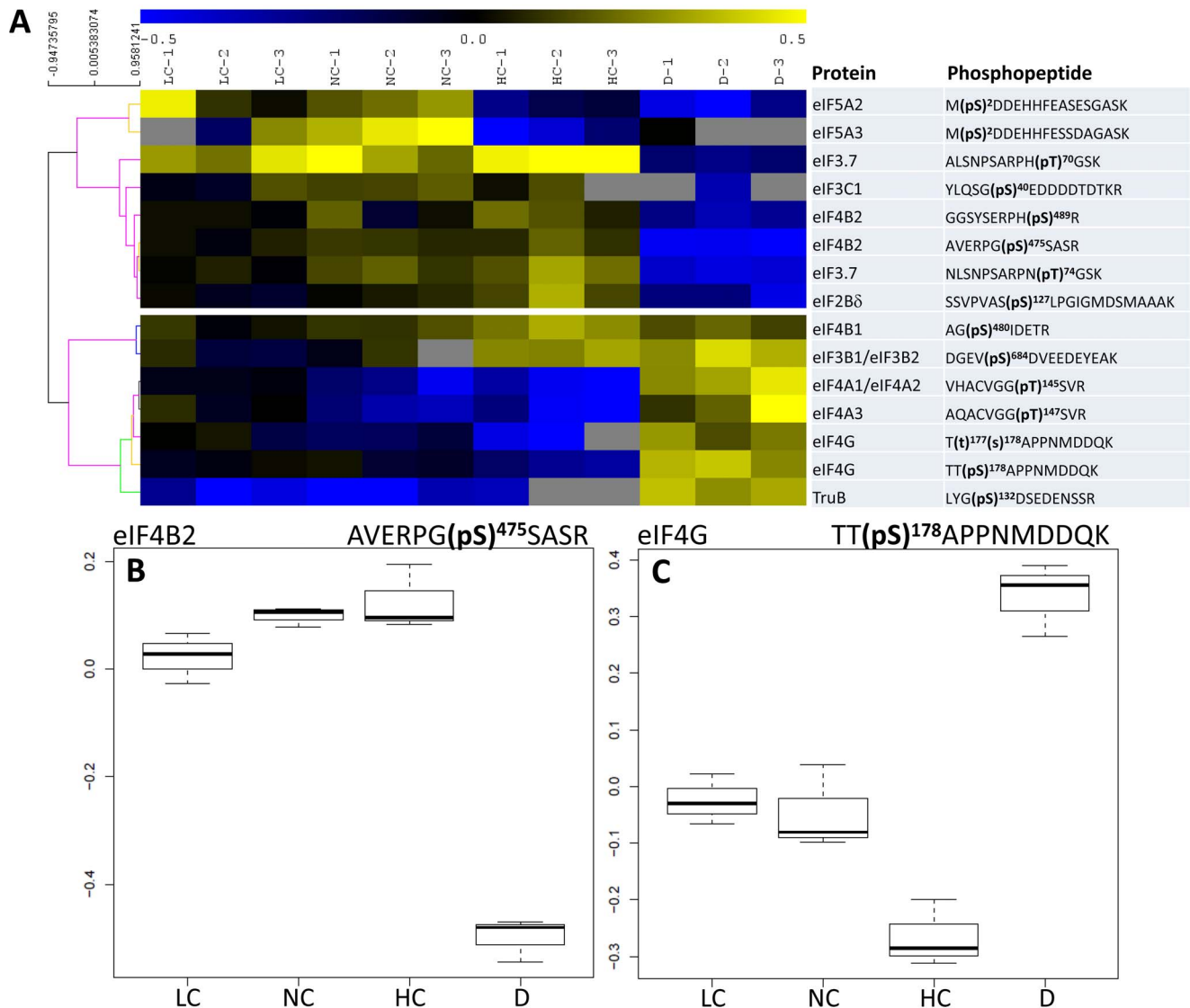


Figure 4. Phosphorylation pattern of initiation factors eIFs. **A**, Heat map representation of the phosphorylation level of significant phosphopeptides. A hierarchical clustering analysis is shown on the left so as to separate photosynthesis or light-stimulated (top) and -inhibited (bottom) phosphorylation events. Unavailable data (non-detected peptides) are indicated with a grey cell. **B** and **C**, Detailed phosphorylation pattern of eIF4B2 and eIF4G. LC, NC, HC and D: low, normal and high CO₂ and darkness.
doi:10.1371/journal.pone.0070692.g004

New Phosphorylation Sites

Most phosphorylation sites in RPs described here (Table S1) are novel, with the notable exception of Ser 231, Ser 237 and Ser 240 in RPS6A/B [8]. We found the new phosphorylation site Ser 229, which cannot be unambiguously attributed to RPS6A or RPS6B (Figure 2). eIF3c is associated with a phosphorylation site at Ser 40, which has been anticipated in *Arabidopsis* using sequence alignment with wheat (Ser 53) [12]. eIF4B is phosphorylated at Ser 422 in mammals but this site does not exist in *Arabidopsis* [35]. We found instead a phosphorylation site at Ser 462 in eIF4B1 and Ser 475 in eIF4B2 (and three other sites, Table 1). The three phosphorylation sites that vary significantly under our conditions (Ser 480 in eIF4B1, Ser 475 and Ser 489 in eIF4B2) seem to be conserved in higher plants (such as *A. lyrata*, *Populus trichocarpa*, *Glycine max* and *Vitis vinifera*). eIF4G appeared to be phosphorylated in the N-ter region as we found phosphorylation sites at Thr 177 and/or Ser 178. However, this region is not associated with a clear

function in translation [29,36]. We further found two new phosphorylation sites (Ser 530 and 1353) which might influence eIF4G activity (these Ser residues might be in regions interacting with eIF3 and eIF4E as in yeast [37]). eIF5A3 has been shown to be phosphorylated at Ser 2 in maize [33,34] and the same site is found here (Table 1).

Translational Control and Photosynthesis

Considering the whole data set obtained here, clear phosphorylation patterns were observed in key actors of translation initiation (RPs, eIFs) likely reflecting stimulation of daytime translation (compared to the dark). There is a considerable literature showing that nitrogen metabolism and nitrate assimilation occur during daytime in leaves (reviewed in [38]) while dark respiration is (partly) fed by protein degradation and amino acid recycling [39]. That is, metabolic imperatives caused by light/dark alternation are so that in leaves, gross protein synthesis and

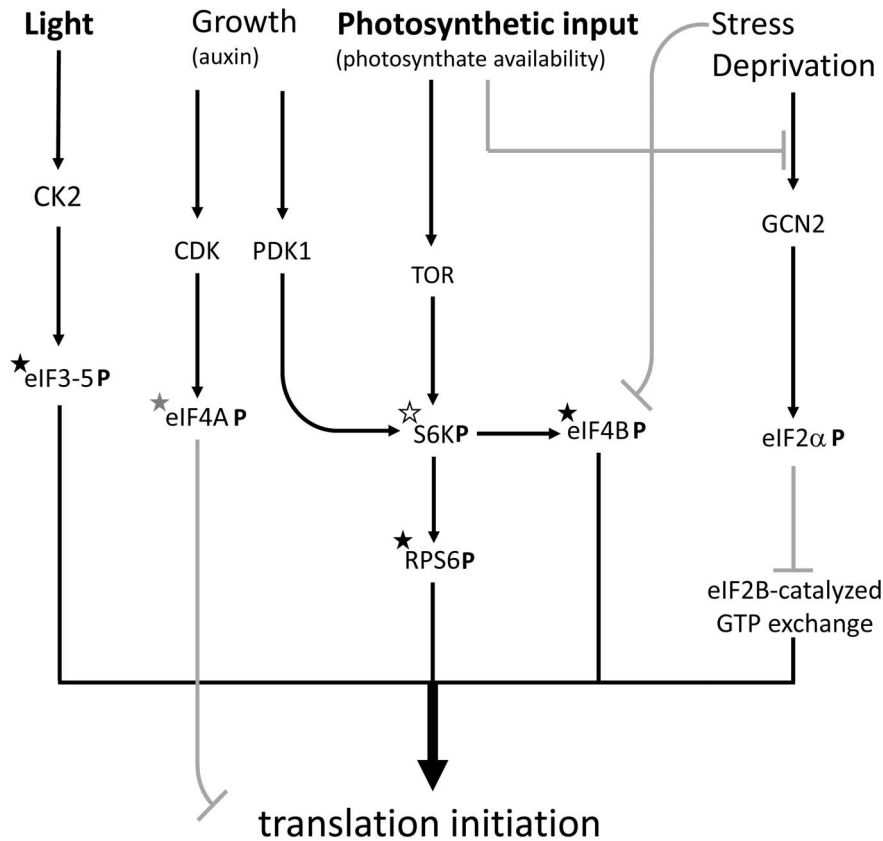


Figure 5. Tentative summary of protein phosphorylation events involved in translation initiation during photosynthesis, with activating (black) and repressing (grey) effects. Phosphorylated proteins are indicated with the symbol P. Those associated with phosphopeptides detected in the present study are indicated with a star, with the phosphorylation level that either correlates (black star), anti-correlates (grey star) or stays constant (white star) with photosynthesis. This figure is simplified and does not mention all molecular actors (such as eIF4G and eIF2B δ).

doi:10.1371/journal.pone.0070692.g005

translational activity is more important in the light. Our results suggest that translation initiation is stimulated via phosphorylation of RP proteins, eIF2B δ , eIF3 and eIF4B and dephosphorylation of repressing sites in eIF4A and eIF4G when photosynthesis increases. The molecular mechanism and rationale of this regulation remain to be elucidated, though. We suggest that important cellular kinases are responsible for this pattern (Figure 5). In fact, eIF2, eIF3c, eIF4B and eIF5 are phosphorylated by CK2 which in turn seems to be activated by light phase duration [40] and photomorphogenesis [41] and thus presumably, might be activated during active photosynthesis. In mammals, eIF4B is phosphorylated by the S6K kinase (which also phosphorylates RPS6) and ORF45 of the herpes virus, and this stimulates translational activity [42]. Despite the fact that the phosphorylated site of mammalian eIF4B is not conserved in plants, eIF4B phosphorylation probably stimulates translation initiation. Furthermore, plants have two S6K isoforms (S6K1 and S6K2) that are activated by PDK1 which is in turn activated by auxin response and growth [43]. S6K is also activated by the TOR-RAPTOR signalling pathway and, perhaps, SnRK1 under specific metabolic conditions (photosynthate and sugar availability) [9,44]. By contrast, GCN2-catalyzed phosphorylation of eIF2 α (from which no phosphopeptide was detected here) is stimulated under deprived or stressful conditions [45]. Taken as a whole, there is probably a balance between the stimulation of translation initiation caused by favourable nutritional conditions (photosyn-

thesis) and the repression caused by cell division (e.g., CDK-dependent phosphorylation of eIF4A, [46]) or stress (e.g., GCN2-catalyzed phosphorylation of eIF2 α) (Fig. 5).

Perspectives

Our understanding of translation initiation in plants is still rather incomplete and further work is needed to disentangle the specific role of individual eIFs and their associated phosphorylation. In that regard, our model in Figure 5 is very crude and probably not fully representative. Future high-throughput sequencing and proteomics are warranted to yield substantial pieces of information on translational control in response to environmental conditions. Our data suggest that natural nutritional conditions influence translation *in folio*. This is probably of prime importance *in situ* (in the field) since changes in CO₂ mole fraction occur quite frequently due to, for example, stomatal closure or diurnal CO₂ changes in the ecosystem atmosphere. Some uncertainty nevertheless remains as to the targets of such a translational regulation: since the use of different eIFs modifies mRNA affinity (e.g., eIF4E versus eIF(iso)4E), the nature of mRNA selected for increased translation during photosynthesis is probably finely adjusted. Future translomics (and polysome) analyses or ¹⁵N-labeling followed by protein-specific isotopic analyses would be required to describe the full translational picture of photosynthesising leaves.

Materials and Methods

Plant Material and Gas-exchange

After sowing on potting mix, *Arabidopsis* (Col-0 ecotype) plantlets were transplanted to individual pots and grown in a controlled environment (growth chamber) under 8:16 h light/dark (short days) at an irradiance of approximately $100 \mu\text{mol m}^{-2} \text{s}^{-1}$, 20/18°C day/night temperature, 65% humidity and nutrient solution (1 g L^{-1} PP14-12-32, [Plant-Prod, Puteaux, France] supplemented with $20 \mu\text{L L}^{-1}$ fertoligo L [Fertil, Boulogne-Billancourt, France]) twice a week. Gas-exchange were carried out with a purpose-built cuvette adapted to three *Arabidopsis* rosettes connected to the sample channel of the Li-Cor 6400 *xt* (Li-Cor, Lincoln, USA). Water vapour in inlet air was fixed (dew point temperature 11.6°C) with a dew-point generator Li-610 (Li-Cor, Lincoln, USA). Air temperature in the chamber was maintained with a water-bath. Leaf rosettes were separated from the below-ground part and soil of the pot by a plexiglass wall (with specific holes for collars) so as to avoid alteration of gas-exchange by soil and root respiration. The upper wall of the leaf cuvette was made of a tight polyvinyl chloride film allowing instant sampling by liquid N₂ spraying. Photosynthesis was allowed to stabilise under the desired CO₂ mole fraction (at $250 \mu\text{mol m}^{-2} \text{s}^{-1}$ PAR) and after 4 hours, rosettes were instantly frozen and stored at -80°C for further analyses. Rosettes sampled in darkness were collected after 4 hours at 380 ppm CO₂ and 2 hours dark-adaptation.

Protein Extraction and In-solution Digestion

Leaf fragments were finely ground with liquid nitrogen. Protein extraction was carried out by using the TCA/acetone method. Briefly, the powder was incubated in a precipitating solution (10% TCA, 0.07 β-mercaptoethanol in acetone) for 1h at -20°C. After centrifugation (19 000 g), the pellet was rinsed three times in 0.07% β-mercaptoethanol in acetone and spin-dried. It was then suspended in a solubilization solution made of 6 M urea, 2 M thiourea, 2% CHAPS (w/v) and 30 mM Tris-HCl pH 7.8 (60 μL/mg) and cell debris were eliminated by centrifugation. Total protein content was determined using the 2-D Quant-kit (GE Healthcare). 2 mg of proteins were reduced by adding DTT (final concentration: 10 mM) and then alkylated by adding iodoacetamide (final concentration: 40 mM). The samples were diluted to 1 M urea by adding 50 mM ammonium bicarbonate. Protein digestion (sequencing grade modified trypsin, Promega) was performed at an enzyme/substrate ratio of 1:30 (w/w) by overnight incubation at 37°C, and stopped by adding 1% formic acid (v/v).

Stable Isotope Dimethyl Labeling

Tryptic peptides were spin-dried and re-suspended in 1 mL of 5% formic acid (v/v). Stable isotope dimethyl labeling was performed according to the on-column procedure described by [47] using formaldehyde or [²H₂]formaldehyde (labeling). Each sample was loaded on a separate SepPak C18 cartridge column (3cc, Waters) and washed with 0.6% acetic acid (v/v). SepPak columns were flushed seven times with 1 mL of the respective labeling reductive reagent (50 mM sodium phosphate buffer pH 7.5, 30 mM NaBH₃CN and 0.2% CH₂O or C²H₂O (v/v)). Samples were eluted with 500 μL of 0.6% acetic acid (v/v) and 80% acetonitrile (v/v). All labelled dimethylated peptides were homogenized to form a reference sample, before being mixed with the unlabeled dimethylated peptides in a 1:1 abundance ratio.

Peptide Fractionation Using Strong Cation Exchange Chromatography (SCX)

Prior to SCX, the dimethyl-labeled peptides were spin-dried and resuspended in 500 μL of solvent A (30% acetonitrile (v/v), 5% formic acid (v/v), pH 2.5). SCX was performed at 200 μL/min using Zorbax BioSCX-Series II columns (0.8-mm inner diameter×50-mm length; 3.5 μm particle size) and a Famos autosampler (LC Packings). After sample loading, the first 17 min were run isocratically at 100% solvent A, followed by an increasing pH gradient using solvent B (30% acetonitrile (v/v), 5% formic acid (v/v), 540 mM ammonium formate, pH 4.7). Twelve SCX fractions per sample were automatically collected using an on-line Probot system (LC Packings).

Selective Enrichment of Phosphopeptides Using Immobilized Metal Ion Affinity Chromatography (IMAC)

SCX fractions were dried and resuspended in 300 μL of solvent C (250 mM acetic acid, 30% acetonitrile (v/v)). Peptides were gently mixed with 80 μL of Phos-Select iron affinity gel (Sigma-Aldrich) and incubated for 2 hours using a tube rotator, as described by [48]. The mixture was transferred into SigmaPrep spin columns (Sigma-Aldrich) and the flow-through fractions containing the non-phosphorylated peptides were collected. Iron affinity gel with bound phosphopeptides was rinsed twice with 200 μL of solvent C, then with double distilled water. The elution of bound phosphopeptides was achieved with 100 μL of solvent D (400 mM NH₄OH, 30% acetonitrile) by centrifugation at 8200 g. Eluted phosphopeptides were dried and kept at -20°C until LC-MS/MS analysis.

LC-MS/MS Analysis

On-line liquid chromatography was performed on a NanoLC-Ultra system (Eksigent). A 4 μL sample was loaded at 7.5 μL/min on a pre-column cartridge (stationary phase: C18 PepMap 100, particles of 5 μm; column: 100 μm i.d., 1 cm length; Dionex) and desalted with 0.1% formic acid in water. After 3 min, the precolumn cartridge was connected to the separating PepMap C18 column (stationary phase C₁₈ PepMap 100, particles of 3 μm; column 75 μm i.d., 150 mm length; Dionex). Buffers were 0.1% formic acid in water (solvent E) and 0.1% formic acid in acetonitrile (solvent F). Peptide separation was achieved using a linear gradient from 5 to 30% F at 300 nL/min. Eluted peptides were analysed with a Q-Exactive mass spectrometer (Thermo Electron) using a nano-electrospray interface (non-coated capillary probe, 10 μm i.d.; New Objective). Peptide ions were analysed using Xcalibur 2.1 with the following data-dependent acquisition steps: (1) full MS scan on a 300 to 1400 range of mass-to-charge ratio (m/z) with a resolution of 70000 and (2) MS/MS (normalized collision energy: 30%; resolution: 17500). Step 2 was repeated for the 8 major ions detected in step 1.

Identification of Peptides and Phosphorylation Sites

Database searches were performed using X!Tandem CY-CLONE (<http://www.thegpm.org/TANDEM>). Cys carboxyamidomethylation and light and heavy dimethylation of peptide N-termini and lysine residues were set as static modifications while Met oxidation and phosphorylation of tyrosine, serine or threonine residues were set as variable modifications. Precursor mass tolerance was 10 ppm and fragment mass tolerance was 0.02 Th. Identifications were performed using the TAIRrelease 8 database (<http://www.uniprot.org/http://www.arabidopsis.org/>). Identified proteins were filtered and grouped using the X!Tandem pipeline v3.2.0 (<http://pappso.inra.fr/bioinfo/>

xtandempipeline/). Data filtering was achieved according to a peptide E value smaller than 0.01. The false discovery rate (FDR) was estimated to 0.92%.

Quantification of Peptides and Phosphorylation Sites

Relative quantification of non-phosphorylated peptides and phosphopeptides was performed using the MassChroQ software [20] by extracting ion chromatograms (XICs) of all identified peptides within a 10 ppm window and by integrating the area of the XIC peak at their corresponding retention time. LC-MS/MS chromatogram alignment was performed by using common MS/MS identifications as landmarks to evaluate retention time deviations along the chromatographic profiles. Alignments were performed within groups of LC-MS/MS runs originating from similar SCX fractions. For each peptide detected in the heavy and light form in a single LC-MS/MS run, a light-to-heavy ratio was computed. To compensate for possible global deviations to 1:1 of the light/heavy ratio (i.e. unequal mixture of heavy and light samples), normalization was performed by centering to 1 the distribution of all ratios within each LC-MS/MS run. Quantitation of protein amounts was performed by averaging centered data obtained from their different peptides. Subsequent statistical

analyses (analysis of variance) were performed on \log_{10} -transformed normalized data.

Supporting Information

Table S1 Eukaryotic initiation factors and ribosomal proteins identified by nanoLC-MS/MS.
(DOCX)

Table S2 Phosphopeptides identified using nanoLC-MS/MS.
(DOCX)

Acknowledgments

The authors thank the Institut Fédératif de Recherche 87, the Labex Saclay Plant Science and the *Agence Nationale de la Recherche*. The present study was carried in the framework of the program *Jeunes Chercheurs*, under contracts no. 08-3300-55 and 12-0001-01.

Author Contributions

Conceived and designed the experiments: EBF GT MH. Performed the experiments: EBF MD. Analyzed the data: EBF MJ GT MH MZ. Wrote the paper: EBF GT.

References

1. Mothes K (1931) Nitrogen metabolism in higher plants. III. Effect of age and water content of leaf. *Planta* 12: 686–731.
2. Bassham JA, Morawiecka B, Kirk M (1964) Protein Synthesis during Photosynthesis. *Biochim Biophys Acta* 90: 542–552.
3. Petracek ME, Dickey LF, Huber SC, Thompson WF (1997) Light-regulated changes in abundance and polyribosome association of ferredoxin mRNA are dependent on photosynthesis. *Plant Cell* 9: 2291–2300.
4. Piques M, Schulze WX, Hohne M, Usadel B, Gibon Y, et al. (2009) Ribosome and transcript copy numbers, polysome occupancy and enzyme dynamics in *Arabidopsis*. *Mol Syst Biol* 5: 314.
5. Escobar-Gutiérrez AJ, Gaudillère J-P (1997) Carbon partitioning in source leaves of peach, a sorbitol-synthesizing species, is modified by photosynthetic rate. *Physiol Plant* 100: 353–360.
6. Reinbothe C, Pollmann S, Reinbothe S (2010) Singlet oxygen signaling links photosynthesis to translation and plant growth. *Trends Plant Sci* 15: 499–506.
7. Scharf K-D, Nover L (1982) Heat-shock-induced alterations of ribosomal protein phosphorylation in plant cell cultures. *Cell* 30: 427–437.
8. Turkina MV, Klang Arstrand H, Vener AV (2011) Differential phosphorylation of ribosomal proteins in *Arabidopsis thaliana* plants during day and night. *PLoS One* 6: e29307.
9. Mahfouz MM, Kim S, Delauney AJ, Verma DP (2006) *Arabidopsis* TARGET OF RAPAMYCIN interacts with RAPTOR, which regulates the activity of S6 kinase in response to osmotic stress signals. *Plant Cell* 18: 477–490.
10. Otterhag L, Gustavsson N, Alsterford M, Pical C, Lehrach H, et al. (2006) *Arabidopsis* PDK1: identification of sites important for activity and downstream phosphorylation of S6 kinase. *Biochimie* 88: 11–21.
11. Muench DG, Zhang C, Dahodwala M (2012) Control of cytoplasmic translation in plants. *RNA* 3: 178–194.
12. Dennis MD, Person MD, Browning KS (2009) Phosphorylation of Plant Translation Initiation Factors by CK2 Enhances the in Vitro Interaction of Multifactor Complex Components. *J Biol Chem* 284: 20615–20628.
13. Dennis MD, Browning KS (2009) Differential Phosphorylation of Plant Translation Initiation Factors by *Arabidopsis thaliana* CK2 Holoenzymes. *J Biol Chem* 284: 20602–20614.
14. Le H, Browning KS, Gallie DR (2000) The phosphorylation state of poly(A)-binding protein specifies its binding to poly(A) RNA and its interaction with eukaryotic initiation factor (eIF) 4F, eIF5A, and eIF4B. *J Biol Chem* 275: 17452–17462.
15. Khan MA, Goss DJ (2004) Phosphorylation States of Translational Initiation Factors Affect mRNA Cap Binding in Wheat. *Biochemistry* 43: 9092–9097.
16. Browning KS (2004) Plant translational initiation factors: it is not easy to be green. *Biochem Soc Trans* 32: 589–591.
17. Browning K (1996) The plant translational apparatus. *Plant Mol Biol* 32: 107–144.
18. Bonhomme L, Valot B, Tardieu F, Zivy M (2012) Phosphoproteome dynamics upon changes in plant water status reveal early events associated with rapid growth adjustment in maize leaves. *Mol Cell Proteomics* 11: 957–972.
19. Craig R, Beavis RC (2004) TANDEM: matching proteins with tandem mass spectra. *Bioinformatics* 20: 1466–1467.
20. Valot B, Langella O, Nano E, Zivy M (2011) MassChroQ: a versatile tool for mass spectrometry quantification. *Proteomics* 11: 3572–3577.
21. Carroll AJ, Heazlewood JL, Ito J, Millar AH (2008) Analysis of the *Arabidopsis* cytosolic ribosome proteome provides detailed insights into its components and their post-translational modification. *Mol Cell Proteomics* 7: 347–369.
22. Mehuyas O (2008) Physiological roles of ribosomal protein S6: one of its kind. *Intl Rev Cell Mol Biol* 268: 1–37.
23. Williams AJ, Werner-Fraczek J, Chang IF, Bailey-Serres J (2003) Regulated phosphorylation of 40S ribosomal protein S6 in root tips of maize. *Plant Physiol* 132: 2086–2097.
24. Chang IF, Szick-Miranda K, Pan S, Bailey-Serres J (2005) Proteomic characterization of evolutionarily conserved and variable proteins of *Arabidopsis* cytosolic ribosomes. *Plant Physiol* 137: 848–862.
25. Deprost D, Yao L, Sormani R, Moreau M, Leterreux G, et al. (2007) The *Arabidopsis* TOR kinase links plant growth, yield, stress resistance and mRNA translation. *EMBO Rep* 8: 864–870.
26. Immanuel TM, Greenwood DR, MacDiarmid RM (2012) A critical review of translation initiation factor eIF2 α kinases in plants – regulating protein synthesis during stress. *Funct Plant Biol* 39: 717–735.
27. Jackson RJ, Hellen CUT, Pestova TV (2010) The mechanism of eukaryotic translation initiation and principles of its regulation. *Nature Rev Mol Cell Biol* 10: 113–127.
28. Webster C, Gaut RL, Browning KS, Ravel JM, Roberts JK (1991) Hypoxia enhances phosphorylation of eukaryotic initiation factor 4A in maize root tips. *J Biol Chem* 266: 23341–23346.
29. Gallie DR, Le H, Caldwell C, Tanguay RL, Hoang NX, et al. (1997) The phosphorylation state of translation initiation factors is regulated developmentally and following heat shock in wheat. *J Biol Chem* 272: 1046–1053.
30. Patrick RM, Browning KS (2012) The eIF4F and eIF5A Complexes of Plants: An Evolutionary Perspective. *Comp Funct Genomics* 2012: 12.
31. Browning KS, Yan TF, Lauer SJ, Aquino LA, Tao M, et al. (1985) Phosphorylation of wheat germ initiation factors and ribosomal proteins. *Plant Physiol* 77: 370–373.
32. Mayberry LK, Allen ML, Nitka KR, Campbell L, Murphy PA, et al. (2011) Plant cap-binding complexes eukaryotic initiation factors eIF4F and eIF5A: molecular specificity of subunit binding. *J Biol Chem* 286: 42566–42574.
33. Lebska M, Ciesielski A, Szymona L, Godecka L, Lewandowska-Gnatowska E, et al. (2010) Phosphorylation of maize eukaryotic translation initiation factor 5A (eIF5A) by casein kinase 2: identification of phosphorylated residue and influence on intracellular localization of eIF5A. *J Biol Chem* 285: 6217–6226.
34. Lewandowska-Gnatowska E, Szymona L, Lebska M, Szczegielniak J, Muszynska G (2011) Phosphorylation of maize eukaryotic translation initiation factor on Ser2 by catalytic subunit CK2. *Mol Cell Biochem* 356: 241–244.
35. Raught B, Peiretti F, Gingras AC, Livingstone M, Shahbazian D, et al. (2004) Phosphorylation of eucaryotic translation initiation factor 4B Ser422 is modulated by S6 kinases. *EMBO J* 23: 1761–1769.
36. Cheng S, Gallie DR (2010) Competitive and noncompetitive binding of eIF4B, eIF4A, and the poly(A) binding protein to wheat translation initiation factor eIF5A. *Biochemistry* 49: 8251–8265.
37. Schütz P, Bumann M, Oberholzer AE, Bieniossek C, Trachsel H, et al. (2008) Crystal structure of the yeast eIF4A-eIF4G complex: an RNA-helicase controlled by protein-protein interactions. *Proc Natl Acad Sci USA* 105: 9564–9569.

38. Stitt M, Müller C, Matt P, Gibon Y, Carillo P, et al. (2002) Steps towards an integrated view of nitrogen metabolism. *J Exp Bot* 53: 959–970.
39. Araújo WL, Tohge T, Ishizaki K, Leaver CJ, Fernie AR (2011) Protein degradation – an alternative respiratory substrate for stressed plants. *Trends Plant Sci* 16: 489–498.
40. Lu SX, Liu H, Knowles SM, Li J, Ma L, et al. (2011) A role for protein kinase casein kinase2 alpha-subunits in the Arabidopsis circadian clock. *Plant Physiol* 157: 1537–1545.
41. Moreno-Romero J, Carme Espunya M, Platara M, Ariño J, Carmen Martínez M (2008) A role for protein kinase CK2 in plant development: evidence obtained using a dominant-negative mutant. *Plant J* 55: 118–130.
42. Kuang E, Fu B, Liang Q, Myoung J, Zhu F (2011) Phosphorylation of Eukaryotic Translation Initiation Factor 4B (EIF4B) by Open Reading Frame 45/p90 Ribosomal S6 Kinase (ORF45/RSK) Signaling Axis Facilitates Protein Translation during Kaposi Sarcoma-associated Herpesvirus (KSHV) Lytic Replication. *J Biol Chem* 286: 41171–41182.
43. Teale WD, Paponov IA, Palme K (2006) Auxin in action: signalling, transport and the control of plant growth and development. *Nat Rev Mol Cell Biol* 7: 847–859.
44. Robaglia C, Thomas M, Meyer C (2012) Sensing nutrient and energy status by SnRK1 and TOR kinases. *Curr Opin Plant Biol* 15: 301–307.
45. Lageix S, Lanet E, Pouch-Pelissier MN, Espagnol MC, Robaglia C, et al. (2008) Arabidopsis eIF2alpha kinase GCN2 is essential for growth in stress conditions and is activated by wounding. *BMC Plant Biol* 8: 134.
46. Pierrat OA, Mikitova V, Bush MS, Browning KS, Doonan JH (2007) Control of protein translation by phosphorylation of the mRNA 5'-cap-binding complex. *Biochem Soc Trans* 35: 1634–1637.
47. Boersema PJ, Raijmakers R, Lemeer S, Mohammed S, Heck AJR (2009) Multiplex peptide stable isotope dimethyl labeling for quantitative proteomics. *Nat Protocols* 4: 484–494.
48. Nühse TS, Bottrill AR, Jones AME, Peck SC (2007) Quantitative phosphoproteomic analysis of plasma membrane proteins reveals regulatory mechanisms of plant innate immune responses. *The Plant Journal* 51: 931–940.